High field cardiac magnetic resonance imaging: a case for ultrahigh field cardiac magnetic resonance

Niendorf, T., Schulz-Menger, J., Paul, K., Huelnhagen, T., Ferrari, V.A., Hodge, R.

This is the final version of the accepted manuscript. The original article has been published in final edited form in:

Circulation Cardiovascular Imaging
2017 JUN ; 10(6): e005460
2017 JUN 13 (first published online: final publication)
doi: 10.1161/CIRCIMAGING.116.005460

Publisher: American Heart Association | Lippincott Williams & Wilkins

A Case for Ultrahigh Field Cardiac Magnetic Resonance

Thoralf Niendorf, Ph.D.[1,2] Jeanette Schulz-Menger M.D.[2,3],

Katharina Paul, Ph.D.[1], Till Huelnhagen, Dipl. Ing.[1],

Victor A. Ferrari, M.D., Ph.D.[4] and Russell Hodge, M.A.[1]

[1)] Berlin Ultrahigh Field Facility (B.U.F.F.), Max-Delbrueck Center for Molecular Medicine in the Helmholtz Association, Berlin, Germany

[2)] DZHK (German Centre for Cardiovascular Research), partner site Berlin, Germany

[3)] Working Group on Cardiovascular Magnetic Resonance, Experimental and Clinical Research Center, a joint cooperation between the Charité Medical Faculty and the Max Delbrück Center for Molecular Medicine in the Helmholtz Association, Berlin, Germany and HELIOS Clinic Berlin-Buch, Department for Cardiology and Nephrology

[4)] Division of Cardiovascular Medicine and Penn Cardiovascular Institute, Perelman School of Medicine, University of Pennsylvania, Philadelphia, USA

Short title: The future of cardiac MR is high field

Address correspondence to:

Thoralf Niendorf,
Berlin Ultrahigh Field Facility (B.U.F.F.)
Max-Delbrueck Center for Molecular Medicine in the Helmholtz Association
Robert-Roessle-Strasse 10
13125 Berlin
Germany
phone: +49 030 9406 4505
fax: +49 030 9406 49178
e-mail: thoralf.niendorf@mdc-berlin.de

word count: 4948

Journal Subject Codes: 10128 imaging
10129 Magnetic Resonance Imaging (MRI)

Magnetic resonance
Magnetic resonance imaging
Cardiovascular research

Key words:
cardiovascular imaging; magnetic resonance; MRI; ultrahigh field; MR technology

Where are we coming from?

For a new technology, high field cardiac MR (CMR, 3.0 Tesla ≤ B_0 ≤7.0 Tesla) has come a long way. Not only has the number of reports referencing clinical applications risen [1, 2] but prices for 3.0 T systems have dropped almost 50% since the beginning of the millenniumand operational and service costs are virtually identical to those of 1.5 T machines. New 3.0 T installations make up about 25% of the total market share and are increasing at an annual growth rate of ~10%. High field comprised approximately ~25 % of the abstracts in CMR submitted to the most recent annual meetings of the Society for Cardiac Magnetic Resonance (SCMR) and the International Society for Magnetic Resonance in Medicine (ISMRM). Large-population studies targeting the heart are now being conducted at 3.0 T, including imaging within the framework of the German National Cohort [3]. The advances in CMR at high magnetic field strengths foreshadow some of the potential benefits to be expected as the technology moves to ultrahigh fields (UHF, B_0 ≥7.0 Tesla).

Where do we stand?

The future of high field CMR has obviously not ended at 3.0 T and is moving higher. Technical barriers are being addressed almost as fast as they appear. Clinical CMR at ultrahigh field strengths is rapidly underway[4-6]. About 15% of sites already equipped with a 7.0 T MR system have begun exploring UHF-CMR, with ~50 peer-reviewed publications on human imaging. Early UHF-CMR applications include imaging and spectroscopy of the heart and large vessels [7-22]. This can be achieved due to the inherent relationship between the signal-to-noise ratio (SNR) and magnetic field strength. In parallel, the field is making remarkable progress with respect to novel radiofrequency (RF) technologies [20, 23, 24] and MR methods that should make clinical UHF-CMR feasible as 7.0 T MR machines become more widely available.

Ultimately, we may see a solution to practical and technical issues that need to be resolved before UHF-CMR could move into clinical settings [25]; but these challenges have always faced new technologies. As is customary, we can expect more pioneering research institutions, university hospitals and large clinics to become early adopters of CMR at 7.0 Tesla and start harvesting knowledge and know-how that will benefit us all. Streamlining hardware and software platforms and making them more robust should permit feasibility studies into CMR on which future applications will be built. These research instruments and activities are dedicated to exploring opportunities for discovery; at some point the knowledge gained could surely justify the cost. This has been the case in the past, and the investment and operating costs of a 7.0 T MR facility can expect to draw on the same types of private-public partnerships, core facility reimbursement models, institutional funding and extramural grants that are traditional mechanisms supporting high-end facilities in many institutes today.

Where can UHF-CMR expect to harvest new discoveries?

It has been extremely challenging to connect the molecular and cellular defects that characterize many cardiac diseases to the level of major organ systems at which they play themselves out. Here MRI has a capacity that is nearly unique among instruments: to simultaneously measure many levels of physiological structure, linking the scales of biologists to those of clinicians, *in vivo*. UHF-CMR stands to bridge a crucial gap in spatiotemporal resolution at a mesoscopic level above that of the cell, a terrain that is crucial to myocardial and pathological processes but has been difficult to explore.

Cardiovascular morphology and cardiac chamber quantification

UHF-MR may help extend the boundaries of CMR by facilitating high spatial resolution imaging of cardiovascular morphology, as demonstrated in Figure 1, derived from black blood imaging of the human heart at 7.0 T. A spatial resolution of 0.9 x 0.9 x 4.0 mm^3 was applied, representing an enhancement by an order of magnitude over the standardized CMR protocols practiced in clinics today [26].

Plaque imaging, arterial wall imaging and carotid wall imaging are applications that perhaps demand highest spatial resolution. Figure 1 depicts preliminary results obtained from 2D dark blood fast spin-echo imaging of the carotid artery wall at 7.0 T using an in-plane spatial resolution of (0.6 x 0.6) mm^2. A spatial resolution of (0.4 × 0.4 × 1.5) mm^3 was demonstrated for the normal carotid vessel wall using T_1 weighted dark blood fast spin-echo imaging at 7.0 T [27]. A quantitative comparison revealed a twofold average gain in SNR (Table 1) [27]. T_1 relaxation time of the normal carotid vessel wall was 1628 ms at 7.0 T (3.0 T: T_1=1227 ms), while a T_2 relaxation time of 46 ms was observed at 7.0 T (3.0 T: T_2=55 ms) [27].

Early studies confirmed that UHF-CMR can be used for cardiac chamber quantification of the left [8, 12, 13] and the right ventricle [16] using high density arrays of RF antennae (Figure 2) [20, 23, 24, 28-30]. These studies reported a SNR increase 2.1-time (Table 1) for 7.0 T versus 1.5 T [12]. This favorable effect produces blood myocardium contrast which is competitive with that obtained for 2D CINE SSFP imaging at 1.5 T, high-quality images with a uniform signal intensity and high blood/myocardium contrast over the entire heart as illustrated in Figure 3 and Video 1 in the online supplemental material. The latter depicts short axis views covering the heart from the apex to the base and demonstrates rather uniform signal intensity across the heart facilitated by a modular 32 channel transceiver loop antenna RF array at 7.0 T[20]. Figure 3 depicts four chamber and short-axis views of the heart obtained with a standardized CMR protocol [26] and compares them with a protocol that enhances spatial resolution. The latter reduces the voxel size from 19.4 mm^3 to ~3.0 mm^3, a six-fold improvement in spatial resolution over a standardized clinical CMR protocol [26]. This fidelity

approaches the relative anatomical spatial resolution - in terms of number of voxels with respect to anatomy – demonstrated for animal models [31]. This achievement is translatable into opportunities for discovery, including the ability to detect subtle myocardial crypts (Figure 4) that often appear in conjunction with hypertrophic cardiomyopathy [32]. High spatial fidelity gradient echo 2D CINE imaging at 7.0T permits the identification of such subtle morphological details in myocardial regions of extended hypertrophy and fibrosis [5]. These structures have not been detectable in this particular myocardial region at current clinical field strengths in the same patient and may yield new insights into developmental aspects of myocardial remodeling [5]. These preliminary results warrant further research in human subjects and animal models to link and validate the UHF-CMR mesoscopic imaging observations with pathologic findings, HCM phenotypes and molecular mechanisms of the disease.

Real-time MRI of the heart

UHF-CMR provides an unprecedented potential for real-time imaging and addressing some of the shortcomings and physiological constraints of traditional assessments of LV and RV structure and function. The accelerated imaging capabilities of free breathing real time imaging of the heart at 7.0 T are demonstrated in Figure 5. The spatial resolution of (1.2 x 1.2 x 6.0) mm^3 and the frame rate of 30 frames per second surpass the requirements established by current clinical protocols for standardized assessments of LV structure and function [26]. The findings from such studies may be extrapolated to clinical CMR studies at lower spatial and temporal resolutions, which may enhance their clinical utility.

Myocardial tissue characterization and phenotyping

UHF-CMR opens new avenues into myocardial tissue characterization and phenotyping by mapping the effective transverse relaxation time T_2^*. The linear relationship between magnetic field strength and microscopic susceptibility effects

makes 7.0 T an appealing avenue for T_2^* mapping [17]. This will permit observing enhanced susceptibility effects by lowering the detection level for abnormal tissue as compared to low field MR, and extending the dynamic range of sensitivity for monitoring T_2^* changes.

By reducing the in-phase inter-echo time from 4.8 ms at 1.5 T to 1.02 ms at 7.0 T, UHF-CMR can acquire multiple gradient echoes [14]. Unlike single cardiac phase T_2^* mapping at lower fields, UHF-CMR permits 2D CINE T_2^* mapping across the entire cardiac cycle. Phase-resolved, high resolution T_2^* maps have been made of the human heart *in vivo* at 7.0 T [14, 22]. Temporal changes in T_2^* across the cardiac cycle are not assessable at 1.5 or 3.0 T due to scan time constraints. CINE T_2^* mapping at 7.0 Tesla accomplishes this, reporting cyclic changes in septal T_2^* with a mean increase of end-systolic T_2^* of about 10% compared to end-diastole [22]. The periodic changes in interventricular septal myocardial T_2^* correlate well with changes in the thickness of the septal wall and the left-ventricular radius throughout the cardiac cycle (Figure 6). Cyclic T_2^* variations were attributed to changes in myocardial blood volume fraction rather than oxygenation, an example of the unique information that temporally resolved MR relaxation mapping can reveal about cardiac (patho)physiology *in vivo* [22].

The first cardiac T_2^* maps made at 7.0 T of hypertrophic cardiomyopathy demonstrate that septal T_2^* is increased in patients compared to healthy controls [4] as illustrated in Figure 6. A mean septal T_2^* of 17. 5 ms for HCM patients and of 13.7 ms for healthy subjects matched by body mass index and age were reported[4]. These findings suggest that T_2^* mapping at UHF could provide an important imaging based biomarker in support of diagnoses and risk stratification in cardiomyopathies.

Heteronuclear MRI for metabolic and nanomolecular probing

The greater spectral resolution and sensitivity gain of UHF-MR helps clinicians and researchers to move beyond conventional ^1H imaging to study other MR nuclei that

are more relevant to cardiac metabolism. The higher magnetic fields permit imaging phosphorous (^{31}P), sodium (^{23}Na), fluorine (^{19}F), carbon (^{13}C), oxygen (^{17}O), potassium (^{39}K), chlorine (^{35}Cl) and other nuclei. Each new substance adds greater dimension to our view of cardiac metabolism, bioenergetics and tissue function in ways that should help us integrate our knowledge of events at the molecular scale and their effects on a higher level.

Sodium MRI (^{23}Na MRI), for example, can provide clearer insights into ion homeostasis. Currently, clinical applications are limited by the rapidly decaying ^{23}Na signal and the low sensitivity of ^{23}Na MRI versus ^{1}H MR. The gain of sensitivity at 7.0 T, permitted three-dimensional ^{23}Na imaging of the entire heart with a spatial resolution of (6 x 6 x 6) mm^3 in clinically acceptable acquisition times of <10 minutes [33]. Information from high fields will very likely be applicable in the reverse direction – new associations revealed by ^{23}Na will shed light on conventionally acquired ^{1}H imaging data and help clinicians interpret observations at lower field strengths. The signal intensity gain at 7.0 T has recently enabled CINE ^{23}Na imaging of the beating heart at a temporal resolution of 100 ms [34] as illustrated in Figure 7. Feasibility studies of ^{23}Na MRI at 7.0 T should reveal the diagnostic value of this tool in distinguishing viable from non-viable tissue in ischemic heart disease patients. It may also offer deeper insights into hypertrophic cardiomyopathy, due to reports that this condition is accompanied by a 33% decrease in Na^+,K^+-ATPase activity and a 40% increase in intracellular Na^+ concentrations.

Potassium ions (K^+) play a vital role in myocardial function. While extracellular K^+ concentrations can easily be estimated from laboratory analysis of blood samples, a method for measuring the intracellular K^+ content *in vivo* is greatly needed and would permit novel insights into pathophysiological processes of cardiac diseases, including arrhythmias. Potassium MRI is quite challenging since the sensitivity is about six orders of magnitude less than that of ^{1}H MRI. The sensitivity gain of 7.0 Tesla will enable for the first time quantitative *in vivo* assessment of the cellular potassium

content in myocardium. This approach opens an entirely new research field of MRI-driven phenotyping as a link to personalized medicine.

Phosphorus MR at higher fields will permit new observations of energy metabolism *in vivo*. The sensitivity gain at ultrahigh magnetic fields has been demonstrated in comparisons between cardiac ^{31}P-MRS at 7.0 T and 3.0 T [19], which highlighted the marked superiority of cardiac ^{31}P spectra at 7.0 T as shown in Figure 8. SNR improvements of 2.6 - 2.8 (Table 1) for phosphocreatine (PCr) together with a reduced standard deviation for the PCr/ATP ratio were observed, permitting enhanced quantification of the phosphocreatine/adenosine triphosphate (ATP) concentration ratio [19]. 7.0 Tesla should quickly become the field strength of choice for probing myocardial energetics with cardiac ^{31}P MR spectroscopy [19]. This conclusion is supported by the first study of this type, performed in a cohort of 25 patients with dilated cardiomyopathy (DCM) [6]. The PCr/ATP ratio was found to be significantly lower in DCM patients than in healthy control subjects (Figure 8). These results are a precursor to broader clinical studies aiming to assess the effect of "energy sparing" drugs in patients with DCM [6].

Fluorine magnetic resonance (^{19}F MR) is a valuable tool for *in vivo* tracking and quantification of fluorine-containing exogenous agents, such as emulsified perfluorcarbon tracer or ^{19}F labeled cells. Natural fluorine is virtually absent in body tissue, so ^{19}MRI yields background-free images with complete signal selectivity and specificity. ^{19}F detection is currently beyond the sensitivity of most clinical apparatus at lower field strengths, due to signal-to-noise constraints related to reproducibility; this is reflected by the low number of reports in the literature to date. UHF-MR can perform ^{19}F MRI *in vivo* through the design of dedicated RF antennae. Applications might include *in vivo* monitoring of the inflammatory response to acute myocardial infarction and early ventricular remodeling, as well as studies of the bioavailability and pharmacokinetics of ^{19}F-containing drugs and ^{19}F-labelled cells.

Vascular UHF-MRI

Another common cardiovascular application of MR that stands to benefit from higher field strengths is the angiography (MRA) of the large vessels. The SNR gain and the reduction in the geometry factor (g-factor) can be used to counter noise amplification caused by the acceleration techniques necessary for real time MRA, in order to achieve high spatiotemporal resolution MRA and for scan time shortening.

UHF-MRA permits larger FOV's along the head-feet direction over current short bore low field MR scanners due to the longer magnet and the better B_0-uniformity along the z-direction. Local transmit/receive RF coil arrays tailored for UHF-CMR support anatomic coverage required for MR of large vessels as demonstrated in Figure 9 (left, center) for a $FOV_{head\text{-}feet}$=35 cm for free breathing real time imaging (spatial resolution=1.2 x 1.2 x 6.0 mm^3) and segmented CINE imaging (spatial resolution=1.1 x 1.1 x 2.5 mm^3) of the human aorta. Another potential application includes large volume coverage, time-resolved phase velocity MRA (4D flow), used to study flow patterns and wall shear stress in large vessels. Aortic 4D flow imaging has recently been demonstrated as feasible at 7.0 T using 1.2 mm isotropic spatial resolution (Figure 9, right) [35]. SNR quantification of 4D aortic flow imaging at 7.0 T revealed 2.2 times the SNR of 3.0 T and 3.8 times the SNR of 1.5 T (Table 1), which is in accordance with theoretical considerations [21]. The baseline SNR advantage of UHF-MR also translates into better spatiotemporal resolution in contrast-enhanced MR angiography. Quantification of contrast enhancement of 4D aortic flow imaging showed that SNR gains achieved by contrast-enhanced versus non-enhanced MRA of the descending aorta were 1.8-fold at 1.5T, 1.7-fold at 3T, and 1.4-fold at 7T[21].

The capabilities of non-contrast UHF-MRA were demonstrated for high spatial resolution (0.45 x 0.45 x 1.2 mm^3) coronary artery imaging (CAI) [18], which revealed enhancements in coronary vessel edge sharpness at 7.0 T over state-of-the-art CAI at 3.0 T. SNR of the RCA blood pool was found to be increased (163 %, Table 1) at 7.0 T versus 3.0 T [10]. These improvements should also benefit coronary vessel wall imaging

including preliminary results obtained with a spatial resolution of 0.86 x 0.86 x 1.2 mm^3 [10].

At ultrahigh magnetic fields the T_1 prolongation of tissue and blood (7.0 T: $T_{1,blood}$=2.09 s, 3.0 T: $T_{1,blood}$=1.65 s, 1.5 T: $T_{1,blood}$=1.48 s) improves the suppression of background tissue signal, enhances the vessel-to-background contrast and provides a better delineation of the vessel lumen for in-flow or time-of-flight (TOF) MRA.

How can UHF-CMR benefit low field CMR?

The increasing flow of knowledge from UHF-CMR technologies and applications are advancing the capabilities of clinical CMR at lower field strengths. The move to 7.0 T should be handled more thoughtfully than the transition from 1.5 T to 3.0 T, which was generally a matter of copy-pasting practices and protocols from a lower field to a higher one.

One area of rethinking concerns developments in RF transmit-receive technology that need to be made in connection with ultrahigh field strengths, which has catalyzed work on high density RF and antenna arrays in conjunction with 7.0 T. Knowledge gained from experience with UHF-CMR can likely be re-applied to 3.0 T. Even though RF inhomogeneities and RF power deposition are somewhat offset at lower field strengths, their affects are still felt in clinical CMR at 1.5 T and 3.0 T. Moving to transmission using local RF coils rather than whole body coils would have a number of advantages at 3.0 T. For example, local RF coil transmission was recently used to acquire accurate cardiac chamber quantification at 3.0 T [36]. Generally, passively conducting peripheral implants can be a contraindication for body coil RF transmission because of their potential for RF power deposition induced heating. A solution would be transmission through local RF coils arranged to exclude peripheral implants from excitation. Conductance problems also arise when CMR is used for image-guided navigation during the manipulation of catheters, another application where local transmission using RF coil arrays is beneficial. They offer additional

benefits in that their efficiency in transmission permits reducing the repetition time (TR) compared to whole body coil transmission. For example, in a recently reported 2D CINE SSFP protocol - the gold standard for cardiac chamber quantification and left ventricular (LV) assessment at lower fields – RF power deposition limits imposed a minimum repetition time of TR=4.7 ms for body coil transmission and TR_{min}=3.8 ms for local surface coil array transmission [36]. This ~20% speed gain will likely be highly significant in real-time assessments of the heart. A decrease in TR facilitated by local RF coil transmission broadens the frequency spectrum of the pass bands in SSFP imaging. At 3.0 T this would be helpful for cardiac chamber quantification and cardiac function assessment, because the off-resonance effects from SSFP are pronounced compared to 1.5 Tesla. Contrary to common experience cardiac 2D CINE SSFP images derived with transmit/receive local surface RF coil array at 3.0 T exhibit rather uniform signal intensity across the heart as demonstrated in Figure 10. The blood/myocardium contrast is clinically acceptable and matches that obtained with body coil transmission in conjunction with a local 32 channel receive coil as illustrated in Figure 10.

Another area to profit from UHF-CMR is research targeted at the development of novel cardiac gating/triggering techniques. The methods most commonly used in clinical CMR currently rely on ECG for gating and triggering, but it is an electrical measurement and therefore subject to interference with electromagnetic fields and magneto-hydrodynamic effects, which is frequently an obstacle to CMR at 3.0 T and becomes worse at higher fields. A suitably simple solution has been found in the form of an MR stethoscope. This instrument comprises three main components: (i) an acoustic sensor that registers the phonocardiogram, (ii) a signal processing unit that detects the first heart tone and transforms it into a trigger signal and (iii) a coupler unit to the MRI system [37]. Acoustic gating is independent of electromagnetic fields, and has been shown to be a robust and safe method of gated/triggered MR in the

clinical setting [37, 38]. This application is a direct product of early UHF-MR research that has already benefitted CMR at 3.0 T and 1.5 T [39].

What obstacles lie on the road to UHF-CMR?

Pushing the boundaries of magnetic field strengths in CMR presents the same safety challenges as the advent of any new clinical technology and must be thoroughly tested for its potential physiological impact and physical effects which arise through the use of ultrahigh magnetic fields. A key to clinical applications will be to deepen our general understanding of the interactions between passive-conducting implants and radiofrequency (RF) fields. An increasing number of patients have implants that might limit their access to UHF-CMR, until they are shown to be safe at $B_0 \geq 7.0$ T. Many such implants have been deemed MR-safe at lower magnetic field strengths, but this will require collecting data about their behaviour when exposed to RF heating in UHF-CMR. The first assessments of RF-induced heating at $B_0 \geq 7.0$ T have been carried out on passive, conducting implants including intracoronary stents and metallic arterial stents. They revealed that the presence of stents did not raise temperatures above the standards established by the International Electrotechnical Commission (IEC) [40].

Fully resolving the safety issue will be complicated a bit by the different thermal properties of novel RF antennae configurations, which usually need to be customized for 7.0 T MRI, the development of parallel transmission techniques, and the wide range of stent geometries that need to be taken into account. An important step was made in a recent study of RF-induced heating of coronary stents at 7.0 T [41] based on electromagnetic field (EMF) simulations which incorporated many different coronary stent configurations. Data from electric fields and local RF power deposition were interpreted as a function of the diameter, length, and position of stents relative to the RF transmission source and their orientation versus the E-field [41]. The results provided a model that can be applied to arbitrary geometries and positions of the stents and the configurations of diverse RF coils, and we have proposed a transfer

function that can predict the EM fields induced in coronary stents [41]. This is a quick way to assess and predict the levels of RF power disposition that will affect a particular stent and configuration. It can be incorporated into state-of-the art SAR prediction methods to estimate the SAR that will be induced in coronary stents and other conductive implants in response to the arbitrary RF pulses used for transmission field shimming or parallel transmission. These criteria should be considered in the design of RF coils to ensure low SAR levels in the vicinity of the stent or to achieve comparable SAR levels in tissues with and without stents [41].

These approaches will support and accelerate current safety assessments of coronary stents and other implants that are commonly used in clinical practice. They will help to show that UHF-CMR is safe – and shape our definitions of what that means. By providing a clearer view of the effects of temperature on tissues, the wider range of field strengths and coil configurations will add to our understanding of the effects of RF energy depositions and provide a more realistic view of factors related to safety, especially where limits should be imposed. This should include SAR estimations but suggests a move towards a more general standard that can be implemented in the upcoming Edition 4 of the IEC 60601-2-33 guideline, which expresses temperature or thermal dose in terms of cumulative equivalent minutes at 43°C (CEM_{43}).

UHF-MR safety assessments must not stop with intracoronary stents. Recent work demonstrated the UHF-MR safety of dental wires [42], ocular tantalum markers [43], cranial fixation plates [44] and investigated experiences with a broad range of passive implants and tattoos [45]. Hip implants and other large passive implants being positioned outside the excitation field of view of the local transmit/receive RF antennae do not constitute a major RF heating issue in UHF-CMR. Further research is required to study the UHF-MR safety of sternal wires.

What will the foreseeable future bring?

Almost 40.000 human examinations have already been performed at 7.0 T without indication that the procedure has acute effects on health [46, 47]. The lion's share of UHF-MR examinations to date has been devoted to the brain and neuroscience, but their potential in cardiovascular research is clear and should result in specific clinical benefits. Each increase in magnetic field strength pushes the boundaries of biomedical imaging and cardiology and provides many other benefits that will help translate basic discoveries to the clinic. Joint efforts between basic scientists, clinicians and their industry colleagues are already exploring new modes for mapping cardiac morphology, function, physiology and metabolism. For every milestone of resolution, speed, or contrast that we pass, new routes are opened between basic research on cell cultures and animal models and applications in the clinic.

UHF-CMR has another dimension that may ultimately expand the uses of MR in entirely new directions. The RF energy deposition that lies at the heart of MR imaging can be used in another way: to deliberately alter temperatures by focusing RF power on precise regions of living tissues. This can be accomplished via an MR antenna array, creating a new tool with the unique ability to exert very focused, controlled changes of temperature. We call this approach thermal magnetic resonance [48, 49] and believe it can give us control over a crucial biological parameter - temperature - that has barely been investigated in cardiology due to technological limitations. There has been no systematic thermal phenotyping of diseased tissues, for example, where changes in structure, metabolism, and cellular content surely produce changes in temperature distribution in meaningful ways. Studies will reveal whether UHF-MR guided targeted RF heating for focal RF ablation can be used to terminate defective electrical pathways in the heart as an alternative approach to today's invasive intracardiac catheterization in the treatment of tachycardia.

The extent to which the high cost of 7.0 Tesla magnets can be lowered will depend on improved workflows and economic and ergonomic changes to hardware, some of which are already underway, such as access to shorter magnets. The first

generation of actively shielded 7.0 T magnets offered a length of approximately 255 cm while the early passively shielded version runs a length of approximately 336 cm. These advances have practical effects on the space required by the machines and the degree of comfort they provide to patients. Next-generation, actively shielded 7.0 T MR systems weigh less than 25 tons and are far more compatible with installations in clinical imaging suites than the very first generation of 7.0 T class systems, which required hundreds of tons of passive shielding.

On the regulatory side, at least one MR vendor is committed to file an application for FDA and CE authorization by 2017, which will be a breakthrough *en route* to broader clinical UHF-MR applications and generate more momentum for clinical pioneers and early clinical adaptors in cardiology. This development is supported by the recent harmonization of the technical standards and guidelines (Amendment 2 to IEC 60601-2-33 am2 Ed. 3.0, medical electrical equipment, particular requirements for the basic safety and essential performance of magnetic resonance equipment for medical diagnosis) of the International Electrotechnical Commission (IEC). This update has lifted the limit on the static magnetic field strength for the first level controlled operating mode from 4.0 Tesla to 8.0 Tesla, taking into account FDA, ICNIRP and other peer-reviewed scientific literature.

We are just at the starting line of UHF-CMR. Pioneering reports on MR physics, careful RF power deposition considerations, and novel RF antenna designs spurred the installation of a 10.5 T whole-body MR system at the Center for Magnetic Resonance Research, University of Minnesota, Minneapolis, USA [50], with a bore size and system architecture that support cardiac MR. The first pioneering reports on body imaging in large animals with a weight of 75 kg at 10.5 T have been released, are highly encouraging and will open a path towards cardiac MR at 10.5 T [50].

Physicists, engineers, and pioneers from related disciplines have already taken further steps into the future, theoretically, with something they are calling Extreme Field MR (EF-MR)[47]. This envisions human MR at 14.0 Tesla and at 20.0 Tesla [51, 52], and is an

important conceptual leap; these fields will span even more of the crucial "resolution gap" in our understanding of human biology. While the first 20 Tesla class MR instruments will likely be devoted to discovery and to proofs-of-principle, findings should guide the best use of lower-resolution imaging techniques at lower magnetic fields. The only thing that could keep the dream of human MR at 14.0 T or 20.0 T from becoming reality would be a lack of conviction to follow the path and see what develops. Failing to do so for fear that the clinics will be left behind is to ignore the entire recent history of cardiac imaging discovery. When an entire community of experts devotes its creative efforts to the task, the gain of knowledge alone will lead to answers for questions that we don't yet even know we should ask.

Are we out of the woods yet?

Viewed at 7.0 Tesla, stimulating anatomical, functional and physiometabolic images have already been obtained from the heart. These advances have generated an excitement in cardiovascular imaging communities and become a driving force for the development of UHF-CMR applications. The remaining challenges should be faced openly in collaborations between forward-thinking researchers, clinical scientists and clinicians. They should be interdisciplinary, inter-institutional and international, as exemplified and spearheaded by the German Ultrahigh Field Network (GUFI), the UK7T network and the high field systems and applications study group of the ISMRM. One of the basic principles of these networks is that such collaborations need to be fair and balanced, because of the true interdisciplinary character of the work and the essential role that collective expertise has played moving the field forward.

The heartening pace of discovery is drawing in new talent and driving a transfer of the results of UHF-CMR research into the clinical arena, with implications for MR physics, biomedical engineering, cardiology, internal medicine, radiology, nephrology, and a wide spectrum of related fields of basic research and clinical

science. From today's base camp, UHF-CMR may look like mountainous heights; inevitably, these peaks will be the low fields of tomorrow. CMR at field strengths of 1.5 T and 3.0 T has produced marvelous clinical achievements; we can certainly expect ultrahigh magnetic fields to produce many more, with benefits in both the low and higher field directions. However, this will only happen if we recognize that moving into ultrahigh fields is more than just a matter of buying magnets and installing them and trying to operate them in "core facilities", armed with the concepts that have guided discovery in the lower fields. The ultimate clinical potential of this game-changing technology is far greater; all that is required is the imagination to apply it. We will always believe that we are at the highest point – until we look up. The goal of such predictions is to provide an exciting destination to aim for and push the field as the ultrahigh field of today might become the low field of tomorrow.

Acknowledgements

The authors wish to acknowledge Celal Oezerdem, Oliver Weinberger, Lukas Winter from the Berlin Ultrahigh Field Facility (B.U.F.F.) at the Max-Delbrueck Center for Molecular Medicine in the Helmholtz Association, Berlin, Germany; Armin Nagel, University of Erlangen, Erlangen, Germany; Christopher Rodgers, Radcliffe Department of Medicine, University of Oxford, Oxford, UK; Sebastian Schmitter, German Metrology Institute, Berlin, Germany and Center for Magnetic Resonance Research, University of Minnesota Medical School, Minneapolis, USA.; who kindly contributed examples of their pioneering work or other valuable assistance.

Funding Sources

This work was supported (in part, TN) by the *Deutsche Zentrum für Herz-Kreislauf-Forschung*, *DZHK* (German Centre for Cardiovascular Research, BER 6.1) and by the *Bundesministerium für Bildung und Forschung, BMBF* (Federal Ministry of Education and Research, Berlin, Germany, FKZ 81Z6100161). Thoralf Niendorf received support by the *Bundesministerium für Bildung und Forschung, BMBF* (Federal Ministry of Education and Research, KMU-innovativ: Medizintechnik MED-373-046). Thoralf Niendorf received support by the *Bundesministerium für Bildung und Forschung, BMBF* (Federal Ministry of Education and Research, Berlin, Germany, FKZ 01QE1501B) and the EUROSTARS program (E! 9340 hearRT-4-EU) cofounded by the European Union Horizon 2020 Framework Programme. Thoralf Niendorf received funding by the individualized medicine (iMED) funding program of the Helmholtz Cross-Program Initiative on Personalized Medicine, Berlin, Germany.

Disclosures

Thoralf Niendorf is founder and CEO of MRI.TOOLS GmbH, Berlin, Germany. Thoralf Niendorf received travel funds from Siemens Healthcare, Erlangen, Germany and Siemens Healthcare, SAS, Saint-Denis cedex, France. Thoralf Niendorf is chair of the Highfield and Applications study group of the International Society of Magnetic Resonance in Medicine. Victor Ferrari is member of the executive committee of the Society for Cardiovascular Magnetic Resonance (Past President); the editorial board of the Journal of Cardiovascular Magnetic Resonance; the editorial board of ACCEL, American College of Cardiology; Chair of the Imaging Council of the American College of Cardiolog and immediate past chair of the Cardiac MR Study Group of the International Society for Magnetic Resonance in Medicine. Jeanette Schulz-Menger is member of the executive committee of the Society for Cardiovascular Magnetic Resonance (Immediate Past President); member of the board of trustees of the International Society of Magnetic Resonance in Medicine and runs research collaboration with Siemens Healthineers, Erlangen, Germany and with CIRCLE CVI, Calgary, Canada.

Tables

Table 1:

Synopsis of gains in signal-to-noise ratio (SNR) obtained for cardiovascular MR applications at 7.0 T versus lower field strengths.

application	imaging technique	SNR gain	note
carotid vessel wall imaging [27]	2D T_1-weighted black blood prepared fast spin-echo	2.0 (versus 3.0 T)	RF coil designs used for reception were optimized for the 7.0 T and 3.0 T setup, 3.0 T and 7.0 T RF coil sensitivity similar at target
cardiac chamber quantification [12]	2D CINE fast gradient echo	2.1 (versus 1.5 T)	different RF coil designs used for signal reception at 7.0 T and 1. 5T, RF coil sensitivity in favour of 1.5 T setup
non-contrast enhanced, time-resolved phase velocity 4D aortic flow imaging [21]	3D free breathing, navigator gated, velocity encoded gradient echo	2.2 (versus 3.0 T) 3.8 (versus 1. 5T)	different RF coil designs used for signal reception at 7.0 T and 3.0 T/1.5T, RF coil sensitivity in favour of 3.0 T/1.5 T setup
coronary MR angiography [10]	3D free breathing, naviga-tor gated and fat suppressed 3D k-space segmented fast gradient echo	1.63 (versus 3.0 T)	different RF coil designs used for signal reception at 7.0 T and 3.0 T, RF coil sensitivity in favour of 3.0 T setup
^{31}P spectroscopy of the septum [19]	UTE-CSI	2.6 - 2.8 (PCr signal) (versus 3.0 T)	same RF coil design used at 7.0 T and 3.0 T

Figure Captions

Figure 1:

Left: Examples of high spatial resolution imaging of cardiac morphology at 7.0 T. These short axis views of the heart were derived from fast spin-echo imaging using a spatial resolution of **top:** (0.9 x 0.9 x 4.0) mm^3 and **bottom:** (0.8 x 0.8 x 3.0) mm^3. **Right:** Full field-of-view and zoomed images of the carotid artery vessel wall acquired with 2D dark blood fast spin-echo imaging at 7.0 T using an in-plane spatial resolution of (0.55 x 0.55) mm^2. For imaging a 4 channel transceiver RF building block (Figure 2d) comprising four loop elements was used for each carotid. The phase setting for each loop element was tailored for enhancing transmission field uniformity around the carotids.

Figure 2:

Four chamber views of the heart of a healthy subject acquired at 7.0 T using **a)** a four channel loop, **b)** an eight channel loop, **c)** a sixteen channel loop, **d)** a thirty-two channel loop and **e)** a sixteen channel bow tie antenna transceiver RF array. For 2D the CINE FLASH acquisitions of the four chamber views a spatial resolution of (1.4 x 1.4. x 4.0) mm^3 was used for all RF array configurations.

Figure 3:

Left) End-diastolic short axis views covering the heart from the apex to the base showing rather uniform signal intensity and no major signal voids. Images were derived from 2D CINE FLASH imaging using a spatial resolution of (1.1 x 1.1 x 2.5) mm^3 and a 16 channel transceiver bow tie antenna RF array at 7.0 T. (The supplemental online video shows a video encompassing all cardiac phases.) **Right)** Four chamber views **(left)** and short axis views **(right)** of the heart derived from 2D CINE FLASH

acquisitions at 7.0 T using a standardized clinical protocol with a spatial resolution of (1.8 x 1.8x6.0) mm^3 **(top)** and an enhanced spatial resolution of (1.1 x 1.1x2.5) mm^3 **(bottom)**. The latter constitutes a six-fold improvement in spatial resolution over the standardized CMR protocol.

Figure 4:

A three chamber view **(left)** and a short axis view **(right)** of the heart of a hypertrophic cardiomyopathy patient showing myocardial crypts (white arrows) in the anteroseptal region of the heart[5]. Images were acquired at 7.0 T using 2D CINE gradient-echo imaging with a spatial resolution of (1.4 x 1.4 x 4.0) mm^3.

Figure 5:

Examples derived from free breathing real time imaging of the heart at 7.0 Tesla: a four-chamber view **(left)**, a mid-ventricular short axis view **(center)** and a two-chamber view of the heart **(right)**. Images were acquired at a rate of 30 frames per second and a spatial resolution of (1.2 x 1.2 x 6.0) mm^3 [23].

Figure 6:

UHF-CMR permits 2D CINE T_2^* mapping across the entire cardiac cycle. **top)** A magnitude image and a T_2*-map of an end-diastolic short axis view of the heart obtained for a healthy subject at 7.0 T. **center)** A magnitude image and a T_2*-map of an end-systolic short axis view of the heart obtained for a patient with hypertrophic cardiomyopathy at 7.0 T. **bottom)** Phase-resolved, high resolution T_2^* mapping at 7.0 T revealed that septal T_2^* correlates with myocardial wall thickness **(left)** and LV inner radius **(right)** in healthy volunteers at 7.0 T[22]. Error bars in scatter plots indicate SEM.

Figure 7:

A CINE series of sodium images of the heart covering the entire cardiac cycle with a temporal resolution of 0.1 s. For data acquisition and reconstruction of the transversal view of the heart, a nominal isotropic spatial resolution of 6 mm^3 was used [34].

Figure 8:

Examples for phosphorous (^{31}P) MR spectroscopy in healthy subjects[19] **(top)** and patients with dilated cardiomyopathy[6] **(bottom)** at 7.0 T (red lines) and at 3.0 T (blue lines). The ^{31}P MR spectra were derived from a myocardial region located in the middle of the interventricular septum of the heart. ^{31}P MRS at 7.0 T provided a substantial SNR advantage ($SNR_{gain,PCr}$=2.6-2.8) over ^{31}P MR spectroscopy at 3.0 T. Image courtesy of Christopher Rodgers, Radcliffe Department of Medicine, University of Oxford, Oxford, UK.

Figure 9:

Examples of large field of view cardiovascular imaging derived from non-contrast enhanced free breathing real time imaging **(left)**, segmented 2D CINE FLASH imaging **(center)** and 4D MR flow imaging **(right)** of the aorta at 7.0 T. The accelerated imaging capabilities at 7.0 T and the anatomical coverage of the 16 channel bow tie antenna array used for transmission and reception (Figure 2) supported free breathing real time imaging of the aorta at a rate of 30 frames per second using highly undersampled radial 2D FLASH with nonlinear inverse reconstruction at a spatial resolution of (1.2 x 1.2 x 6.0) mm^3. For comparison conventional, segmented 2D CINE FLASH imaging of the same slice was conducted with an in-plane spatial resolution of (1.1 x 1.1 x 2.5) mm^3. The real time and the 2D CINE FLASH images of the aorta demonstrate the 35 cm anatomic coverage of the 16 channel bow tie antenna array along the head-feet direction including. **Right:** Pathline visualization of

blood velocity within the human aorta at t=306 ms relative to R-wave of the ECG signal. Data were obtained from 4D flow measurements at 7.0 T using 1.2 mm isotropic spatial and 40.8 ms temporal resolution. 4D flow image **(right)** courtesy of Sebastian Schmitter, Germany Metrology Institute, Berlin, Germany and Center for Magnetic Resonance Research, University of Minnesota Medical School, Minneapolis, USA.

Figure 10:

Four chamber and two chamber views of the heart of a healthy human subject obtained with 2D CINE SSFP imaging at 3.0 T. For CMR a local 4 channel surface transceiver RF coil array **(left)** was used. As a comparison, traditional body RF coil transmission was used in conjunction with a local 4 channel receive RF coil array **(middle)** or with a local 32 channel receive RF coil array **(right)** [36]. The uniformity of signal intensity across the heart and the blood/myocardium contrast obtained with local surface coil transmission match that obtained with body coil transmission.

References

1. Oshinski JN, Delfino JG, Sharma P, Gharib AM, Pettigrew RI. Cardiovascular magnetic resonance at 3.0 t: Current state of the art. *J Cardiovasc Magn Reson*. 2010;12:55

2. Rajiah P, Bolen MA. Cardiovascular mr imaging at 3 t: Opportunities, challenges, and solutions. *Radiographics*. 2014;34:1612-1635

3. Bamberg F, Kauczor HU, Weckbach S, Schlett CL, Forsting M, Ladd SC, Greiser KH, Weber MA, Schulz-Menger J, Niendorf T, Pischon T, Caspers S, Amunts K, Berger K, Bulow R, Hosten N, Hegenscheid K, Kroncke T, Linseisen J, Gunther M, Hirsch JG, Kohn A, Hendel T, Wichmann HE, Schmidt B, Jockel KH, Hoffmann W, Kaaks R, Reiser MF, Volzke H. Whole-body mr imaging in the german national cohort: Rationale, design, and technical background. *Radiology*. 2015:142242

4. Huelnhagen T, Hezel F, Pohlmann A, Graessl A, Rieger J, Lysiak D, Thalhammer C, Kellman P, Prothmann M, Schulz Menger J, Niendorf T. High spatial resolution myocardial t2* mapping at 7.0 t reveals differences between healthy volunteers and patients with hypertrophic cardiomyopathy. *23rd Annual Meeting of the International Society of Magnetic Resonance in Medicine*. 2015:2599

5. Prothmann M, von Knobelsdorff-Brenkenhoff F, Topper A, Dieringer MA, Shahid E, Graessl A, Rieger J, Lysiak D, Thalhammer C, Huelnhagen T, Kellman P, Niendorf T, Schulz-Menger J. High spatial resolution cardiovascular magnetic resonance at 7.0 tesla in patients with hypertrophic cardiomyopathy - first experiences: Lesson learned from 7.0 tesla. *PLoS One*. 2016;11:e0148066

6. Stoll VM, Clarke WT, Levelt E, Liu A, Myerson SG, Robson MD, Neubauer S, Rodgers CT. Dilated cardiomyopathy: Phosphorus 31 mr spectroscopy at 7 t. *Radiology*. 2016:152629

7. Snyder CJ, DelaBarre L, Metzger GJ, van de Moortele PF, Akgun C, Ugurbil K, Vaughan JT. Initial results of cardiac imaging at 7 tesla. *Magn Reson Med*. 2009;61:517-524

8. Brandts A, Westenberg JJ, Versluis MJ, Kroft LJ, Smith NB, Webb AG, de Roos A. Quantitative assessment of left ventricular function in humans at 7 t. *Magn Reson Med*. 2010;64:1471-1477

9. van Elderen SG, Versluis MJ, Webb AG, Westenberg JJ, Doornbos J, Smith NB, de Roos A, Stuber M. Initial results on in vivo human coronary mr angiography at 7 t. *Magn Reson Med*. 2009;62:1379-1384

10. van Elderen SG, Versluis MJ, Westenberg JJ, Agarwal H, Smith NB, Stuber M, de Roos A, Webb AG. Right coronary mr angiography at 7 t: A direct quantitative and qualitative comparison with 3 t in young healthy volunteers. *Radiology*. 2010;257:254-259

11. Niendorf T, Sodickson DK, Krombach GA, Schulz-Menger J. Toward cardiovascular mri at 7 t: Clinical needs, technical solutions and research promises. *Eur Radiol*. 2010;20:2806-2816

12. von Knobelsdorff-Brenkenhoff F, Frauenrath T, Prothmann M, Dieringer MA, Hezel F, Renz W, Kretschel K, Niendorf T, Schulz-Menger J. Cardiac chamber quantification using magnetic resonance imaging at 7 tesla--a pilot study. *Eur Radiol*. 2010;20:2844-2852

13. Suttie JJ, Delabarre L, Pitcher A, van de Moortele PF, Dass S, Snyder CJ, Francis JM, Metzger GJ, Weale P, Ugurbil K, Neubauer S, Robson M, Vaughan T. 7 tesla (t) human cardiovascular magnetic resonance imaging using flash and ssfp to assess cardiac function: Validation against 1.5 t and 3 t. *NMR Biomed*. 2012;25:27-34

14. Hezel F, Thalhammer C, Waiczies S, Schulz-Menger J, Niendorf T. High spatial resolution and temporally resolved t2* mapping of normal human myocardium at 7.0 tesla: An ultrahigh field magnetic resonance feasibility study. *PLoS One*. 2012;7:e52324

15. Niendorf T, Graessl A, Thalhammer C, Dieringer MA, Kraus O, Santoro D, Fuchs K, Hezel F, Waiczies S, Ittermann B, Winter L. Progress and promises of human cardiac magnetic resonance at ultrahigh fields: A physics perspective. *J Magn Reson*. 2013;229:208-222

16. von Knobelsdorff-Brenkenhoff F, Tkachenko V, Winter L, Rieger J, Thalhammer C, Hezel F, Graessl A, Dieringer MA, Niendorf T, Schulz-Menger J. Assessment of the right ventricle with cardiovascular magnetic resonance at 7 tesla. *J Cardiovasc Magn Reson*. 2013;15:23

17. Meloni A, Hezel F, Positano V, Keilberg P, Pepe A, Lombardi M, Niendorf T. Detailing magnetic field strength dependence and segmental artifact distribution of myocardial effective transverse relaxation rate at 1.5, 3.0, and 7.0 t. *Magn Reson Med*. 2014;71:2224-2230

18. Bizino MB, Bonetti C, van der Geest RJ, Versluis MJ, Webb AG, Lamb HJ. High spatial resolution coronary magnetic resonance angiography at 7 t: Comparison with low spatial resolution bright blood imaging. *Invest Radiol*. 2014;49:326-330

19. Rodgers CT, Clarke WT, Snyder C, Vaughan JT, Neubauer S, Robson MD. Human cardiac 31p magnetic resonance spectroscopy at 7 tesla. *Magn Reson Med*. 2014;72:304-315

20. Graessl A, Renz W, Hezel F, Dieringer MA, Winter L, Oezerdem C, Rieger J, Kellman P, Santoro D, Lindel TD, Frauenrath T, Pfeiffer H, Niendorf T. Modular 32-channel transceiver coil array for cardiac mri at 7.0t. *Magn Reson Med*. 2014;72:276-290

21. Hess AT, Bissell MM, Ntusi NA, Lewis AJ, Tunnicliffe EM, Greiser A, Stalder AF, Francis JM, Myerson SG, Neubauer S, Robson MD. Aortic 4d flow: Quantification of signal-to-noise ratio as a function of field strength and contrast enhancement for 1.5t, 3t, and 7t. *Magn Reson Med*. 2015;73:1864-1871

22. Huelnhagen T, Hezel F, Serradas Duarte T, Pohlmann A, Oezerdem C, Flemming B, Seeliger E, Prothmann M, Schulz-Menger J, Niendorf T. Myocardial effective transverse relaxation time t2* correlates with left ventricular wall thickness: A 7.0 t mri study. *Magn Reson Med*. 2016, (**2016 Jun 25. doi: 10.1002/mrm.26312. [epub ahead of print] PMID: 27342430**

23. Oezerdem C, Winter L, Graessl A, Paul K, Els A, Weinberger O, Rieger J, Kuehne A, Dieringer M, Hezel F, Voit D, Frahm J, Niendorf T. 16-channel bow tie antenna transceiver array for cardiac mr at 7.0 tesla. *Magn Reson Med*. 2016;75:2553-2565

24. Thalhammer C, Renz W, Winter L, Hezel F, Rieger J, Pfeiffer H, Graessl A, Seifert F, Hoffmann W, von Knobelsdorff-Brenkenhoff F, Tkachenko V, Schulz-Menger J, Kellman P, Niendorf T. Two-dimensional sixteen channel transmit/receive coil array for cardiac mri at 7.0 t: Design, evaluation, and application. *J Magn Reson Imaging*. 2012;36:847-857

25. Niendorf T, Paul K, Oezerdem C, Graessl A, Klix S, Huelnhagen T, Hezel F, Rieger J, Waiczies H, Frahm J, Nagel AM, Oberacker E, Winter L. W(h)ither human cardiac and body magnetic resonance at ultrahigh fields? Technical advances, practical considerations, applications, and clinical opportunities. *NMR Biomed*. 2016;29:1173-1197

26. Kramer CM, Barkhausen J, Flamm SD, Kim RJ, Nagel E. Standardized cardiovascular magnetic resonance (cmr) protocols 2013 update. *J Cardiovasc Magn Reson*. 2013;15:91

27. Koning W, de Rotte AA, Bluemink JJ, van der Velden TA, Luijten PR, Klomp DW, Zwanenburg JJ. Mri of the carotid artery at 7 tesla: Quantitative comparison with 3 tesla. *J Magn Reson Imaging*. 2015;41:773-780

28. Dieringer MA, Renz W, Lindel T, Seifert F, Frauenrath T, von Knobelsdorff-Brenkenhoff F, Waiczies H, Hoffmann W, Rieger J, Pfeiffer H, Ittermann B, Schulz-Menger J, Niendorf T. Design and application of a four-channel transmit/receive surface coil for functional cardiac imaging at 7t. *J Magn Reson Imaging*. 2011;33:736-741

29. Winter L, Kellman P, Renz W, Grassl A, Hezel F, Thalhammer C, von Knobelsdorff-Brenkenhoff F, Tkachenko V, Schulz-Menger J, Niendorf T. Comparison of three multichannel transmit/receive radiofrequency coil configurations for anatomic and functional cardiac mri at 7.0t: Implications for clinical imaging. *Eur Radiol*. 2012;22:2211-2220

30. Grassl A, Winter L, Thalhammer C, Renz W, Kellman P, Martin C, von Knobelsdorff-Brenkenhoff F, Tkachenko V, Schulz-Menger J, Niendorf T. Design, evaluation and application of an eight channel transmit/receive coil array for cardiac mri at 7.0 t. *Eur J Radiol*. 2013;82:752-759

31. Wagenhaus B, Pohlmann A, Dieringer MA, Els A, Waiczies H, Waiczies S, Schulz-Menger J, Niendorf T. Functional and morphological cardiac magnetic resonance imaging of mice using a cryogenic quadrature radiofrequency coil. *PLoS One*. 2012;7:e42383

32. Child N, Muhr T, Sammut E, Dabir D, Ucar EA, Bueser T, Gill J, Carr-White G, Nagel E, Puntmann VO. Prevalence of myocardial crypts in a large retrospective cohort study by cardiovascular magnetic resonance. *J Cardiovasc Magn Reson*. 2014;16:66

33. Graessl A, Ruehle A, Waiczies H, Resetar A, Hoffmann SH, Rieger J, Wetterling F, Winter L, Nagel AM, Niendorf T. Sodium mri of the human heart at 7.0 t: Preliminary results. *NMR Biomed*. 2015;28:967-975

34. Resetar A, Hoffmann SH, Graessel A, Winter L, Waiczies H, Ladd ME, Niendorf T, Nagel AM. Retrospectively-gated cine na imaging of the heart at 7.0tesla using density-adapted 3d projection reconstruction. *Magn Reson Imaging*. 2015

35. Schmitter S, Schnell S, Ugurbil K, Markl M, Van de Moortele PF. Towards high-resolution 4d flow mri in the human aorta using kt-grappa and b1+ shimming at 7t. *J Magn Reson Imaging*. 2016;44:486-499

36. Weinberger O, Winter L, Dieringer MA, Els A, Oezerdem C, Rieger J, Kuehne A, Cassara AM, Pfeiffer H, Wetterling F, Niendorf T. Local multi-channel rf surface coil versus body rf coil transmission for cardiac magnetic resonance at 3 tesla: Which configuration is winning the game? *PLoS One*. 2016;11:e0161863

37. Frauenrath, Tobias, Niendorf, Thoralf, Kob, Malte. Acoustic method for synchronization of magnetic resonance imaging (mri). *Acta Acustica united with Acustica*. 2008;94:148-155

38. Frauenrath T, Hezel F, Renz W, d'Orth Tde G, Dieringer M, von Knobelsdorff-Brenkenhoff F, Prothmann M, Schulz Menger J, Niendorf T. Acoustic cardiac triggering: A practical solution for synchronization and gating of cardiovascular magnetic resonance at 7 tesla. *J Cardiovasc Magn Reson*. 2010;12:67

39. Becker M, Frauenrath T, Hezel F, Krombach GA, Kremer U, Koppers B, Butenweg C, Goemmel A, Utting JF, Schulz-Menger J, Niendorf T. Comparison of left ventricular function assessment using phonocardiogram- and electrocardiogram-triggered 2d ssfp cine mr imaging at 1.5 t and 3.0 t. *Eur Radiol*. 2010;20:1344-1355

40. Santoro D, Winter L, Muller A, Vogt J, Renz W, Ozerdem C, Grassl A, Tkachenko V, Schulz-Menger J, Niendorf T. Detailing radio frequency heating induced by coronary stents: A 7.0 tesla magnetic resonance study. *PLoS One*. 2012;7:e49963

41. Winter L, Oberacker E, Özerdem C, Ji Y, von Knobelsdorff-Brenkenhoff F, Weidemann G, Ittermann B, Seifert F, Niendorf T. On the rf heating of coronary stents at 7.0 tesla mri. *Magnetic Resonance in Medicine*. 2015;74:999-1010

42. Wezel J, Kooij BJ, Webb AG. Assessing the mr compatibility of dental retainer wires at 7 tesla. *Magn Reson Med*. **2014;72:1191-8**

43. Oberacker E, Paul K, Huelnhagen T, Oezerdem C, Winter L, Pohlmann A, Boehmert L, Stachs O, Heufelder J, Weber A, Rehak M, Seibel I, Niendorf T. Magnetic resonance safety and compatibility of tantalum markers used in proton beam therapy for intraocular tumors: A 7.0 tesla study. *Magn Reson Med*. 2016; **doi: 10.1002/mrm.26534. [Epub ahead of print] PMID: 27851881**

44. Kraff O, Wrede KH, Schoemberg T, Dammann P, Noureddine Y, Orzada S, Ladd ME, Bitz AK. Mr safety assessment of potential rf heating from cranial fixation plates at 7 t. *Med Phys*. 2013;40:042302

45. Noureddine Y, Bitz AK, Ladd ME, Thurling M, Ladd SC, Schaefers G, Kraff O. Experience with magnetic resonance imaging of human subjects with passive implants and tattoos at 7 t: A retrospective study. *MAGMA*. 2015;28:577-590

46. Winter L, Niendorf T. Electrodynamics and radiofrequency antenna concepts for human magnetic resonance at 23.5 t (1 ghz) and beyond. *MAGMA*. 2016;29:641-656

47. Niendorf T, Barth M, Kober F, Trattnig S. From ultrahigh to extreme field magnetic resonance: Where physics, biology and medicine meet. *MAGMA*. 2016;29:309-311

48. Winter L, Özerdem C, Hoffmann W, Santoro D, Müller A, Waiczies H, Seemann R, Graessl A, Wust P, Niendorf T, Yacoub E. Design and evaluation of a hybrid radiofrequency applicator for magnetic resonance imaging and rf induced hyperthermia: Electromagnetic field simulations up to 14.0 tesla and proof-of-concept at 7.0 tesla. *PLoS ONE*. 2013;8:e61661

49. Winter L, Oezerdem C, Hoffmann W, van de Lindt T, Periquito J, Ji Y, Ghadjar P, Budach V, Wust P, Niendorf T. Thermal magnetic resonance: Physics considerations and electromagnetic field simulations up to 23.5 tesla (1ghz). *Radiat Oncol*. 2015;10:201

50. Erturk MA, Wu X, Eryaman Y, Van de Moortele PF, Auerbach EJ, Lagore RL, DelaBarre L, Vaughan JT, Ugurbil K, Adriany G, Metzger GJ. Toward imaging the body at 10.5 tesla. *Magn Reson Med*. 2017;77:434-443

51. Winter L, Niendorf T. Electrodynamics and radiofrequency antenna concepts for human magnetic resonance at 23.5 t (1 ghz) and beyond. *MAGMA*. 2016; **29:641-56**

52. Budinger TF, Bird MD, Frydman L, Long JR, Mareci TH, Rooney WD, Rosen B, Schenck JF, Schepkin VD, Sherry AD, Sodickson DK, Springer CS, Thulborn KR, Ugurbil K, Wald LL. Toward 20 t magnetic resonance for human brain studies: Opportunities for discovery and neuroscience rationale. *MAGMA*. 2016;29:617-639

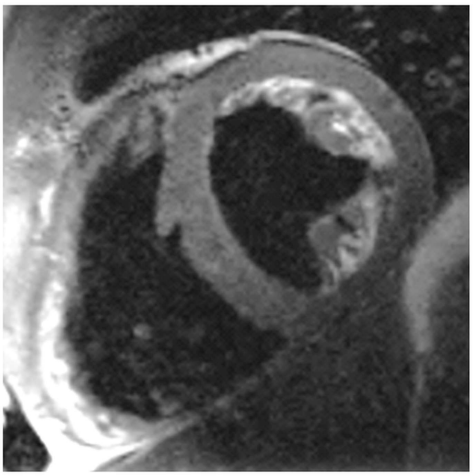

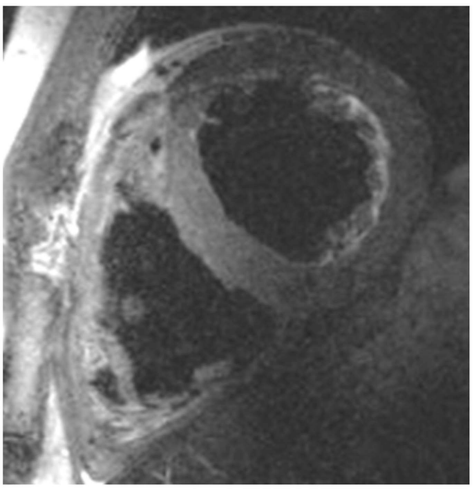

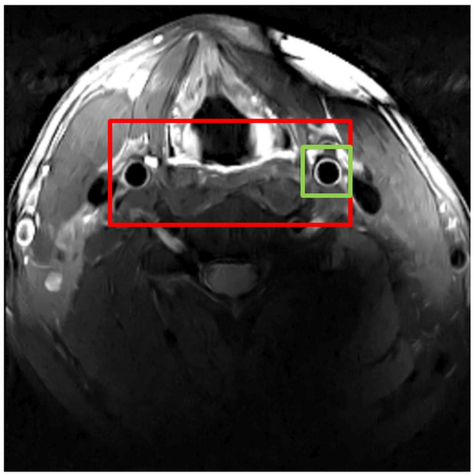

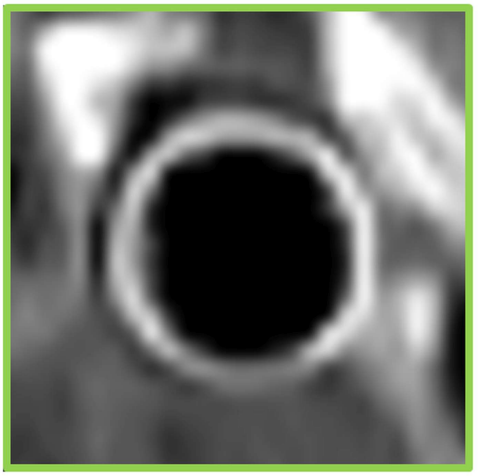

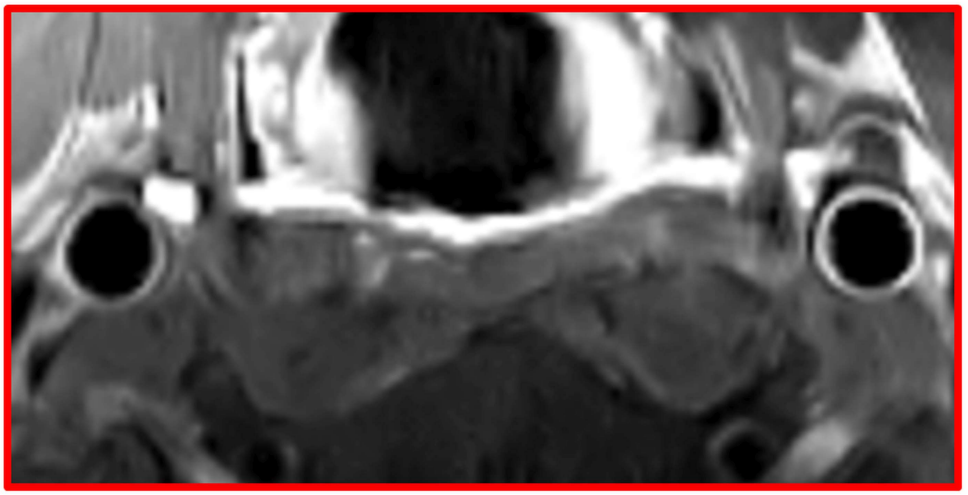

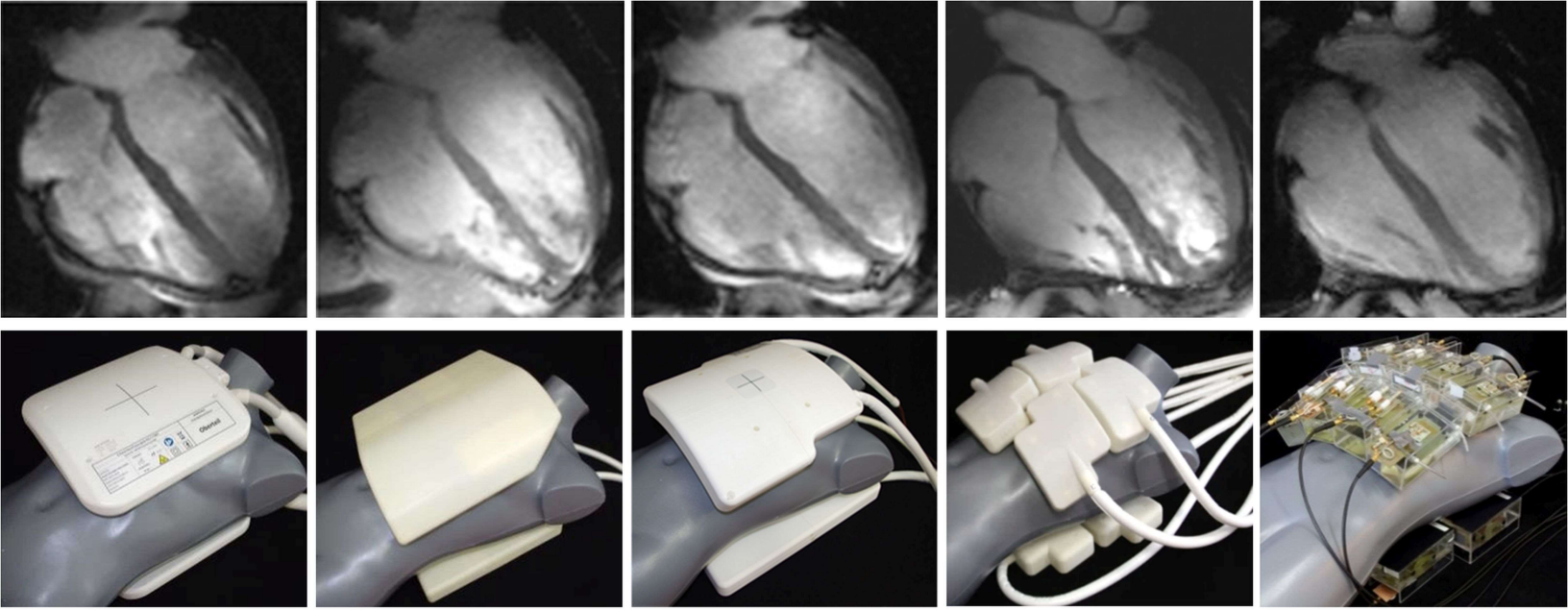

a) four channel TX/RX loop array

b) eight channel TX/RX loop array

c) sixteen channel TX/RX loop array

d) thirty two channel TX/RX loop array

e) 16 channel TX/RX bow tie array

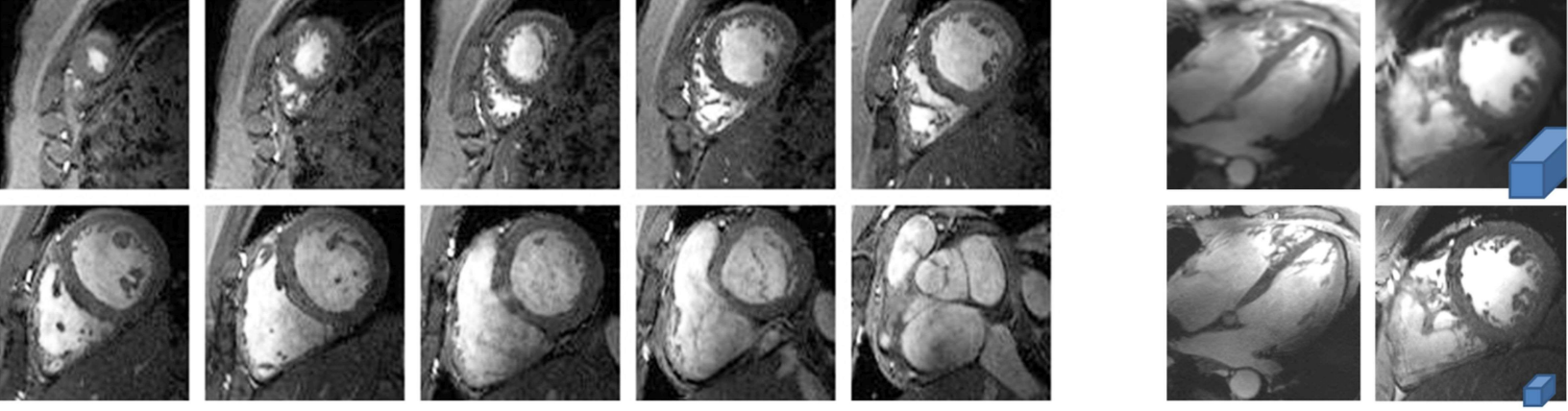

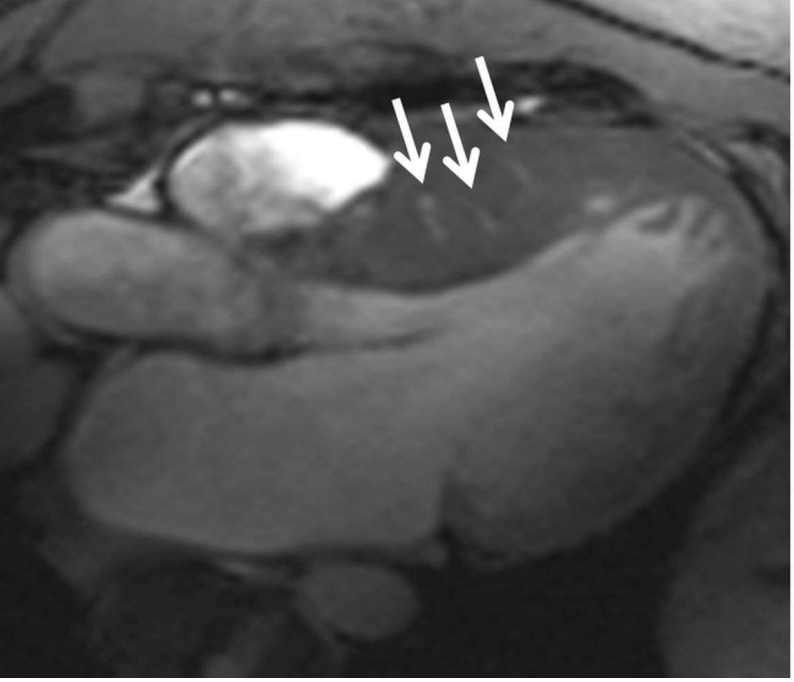

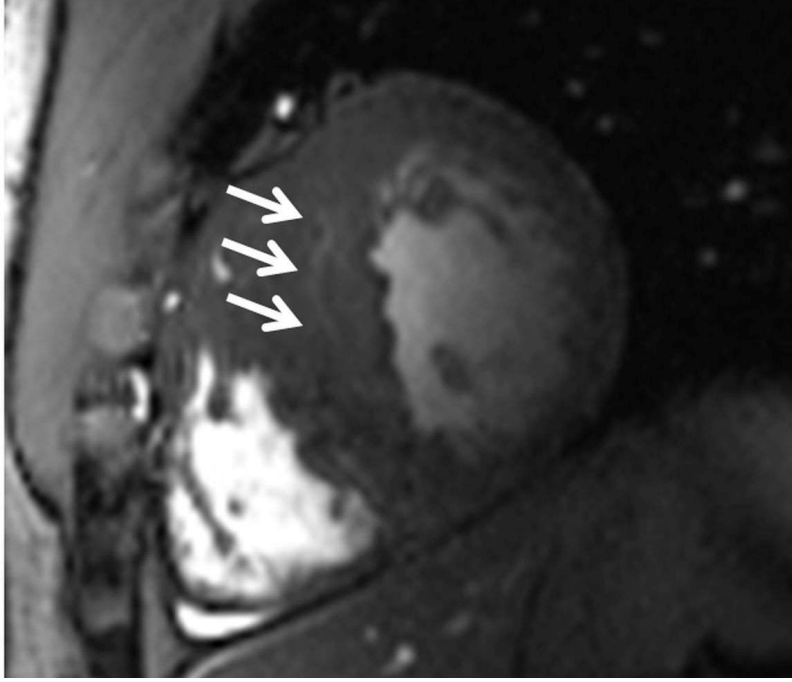

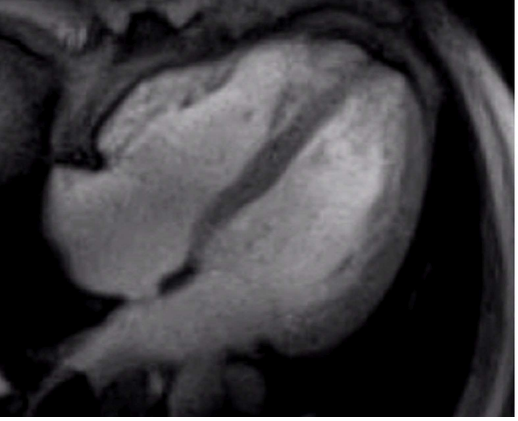

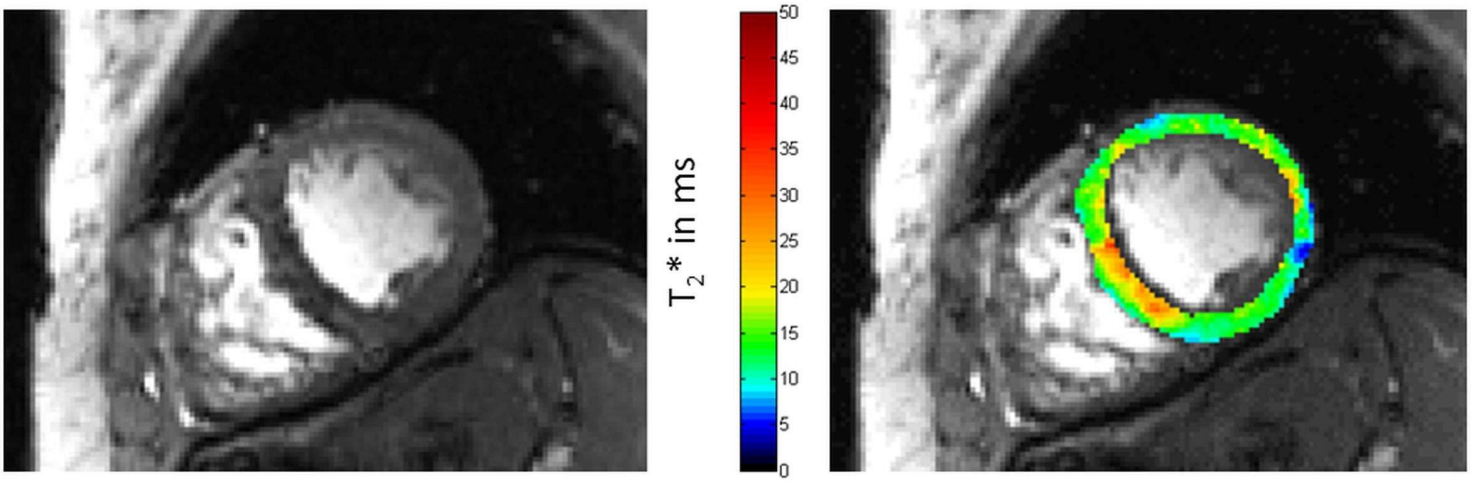
T_2* in ms
50
45
40
35
30
25
20
15
10
5
0

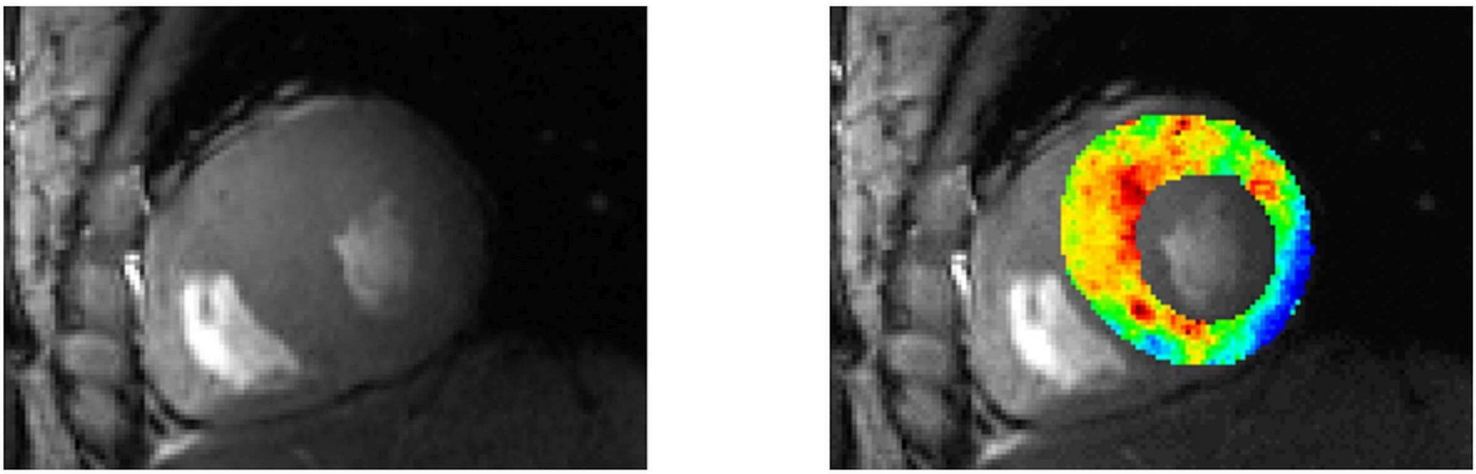

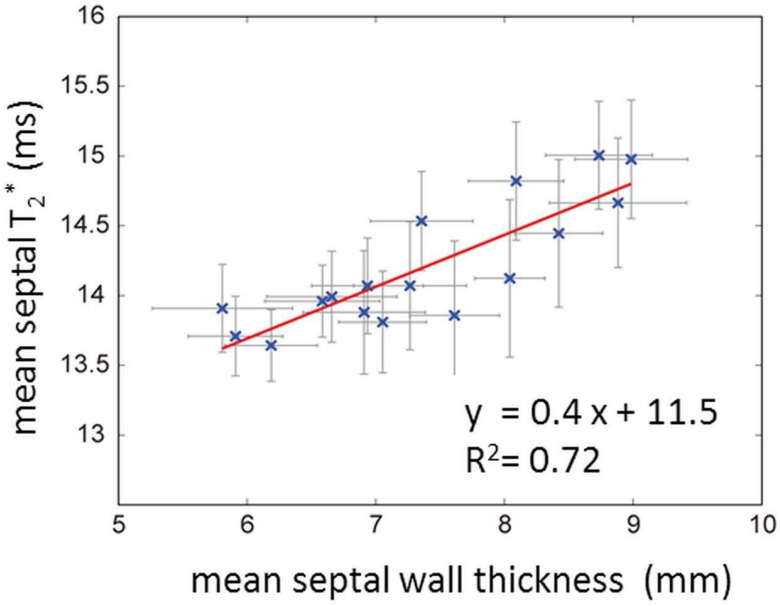
mean septal T_2^* (ms)
16
15.5
15
14.5
14
13.5
13
5
6
7
8
9
10
y = 0.4 x + 11.5
R^2= 0.72
mean septal wall thickness (mm)

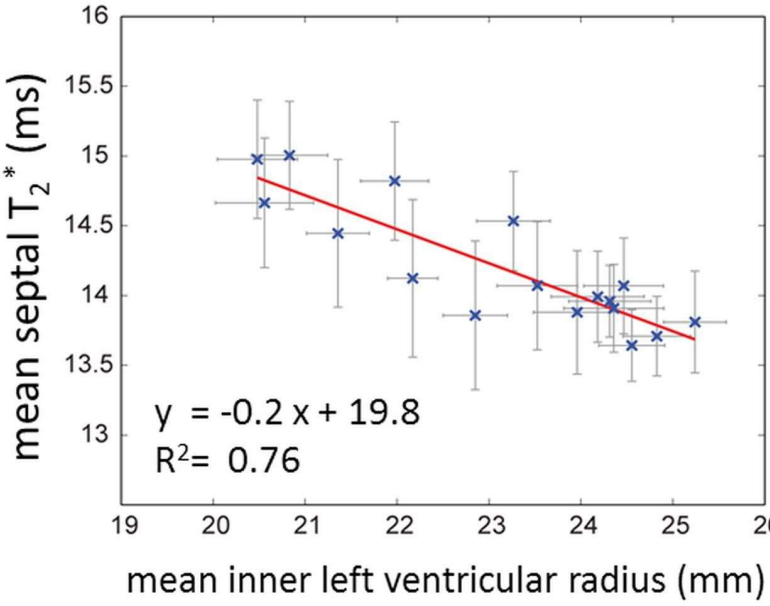
mean septal T_2^* (ms)
16
15.5
15
14.5
14
13.5
13
19
20
21
22
23
24
25
26
y = -0.2 x + 19.8
R^2= 0.76
mean inner left ventricular radius (mm)

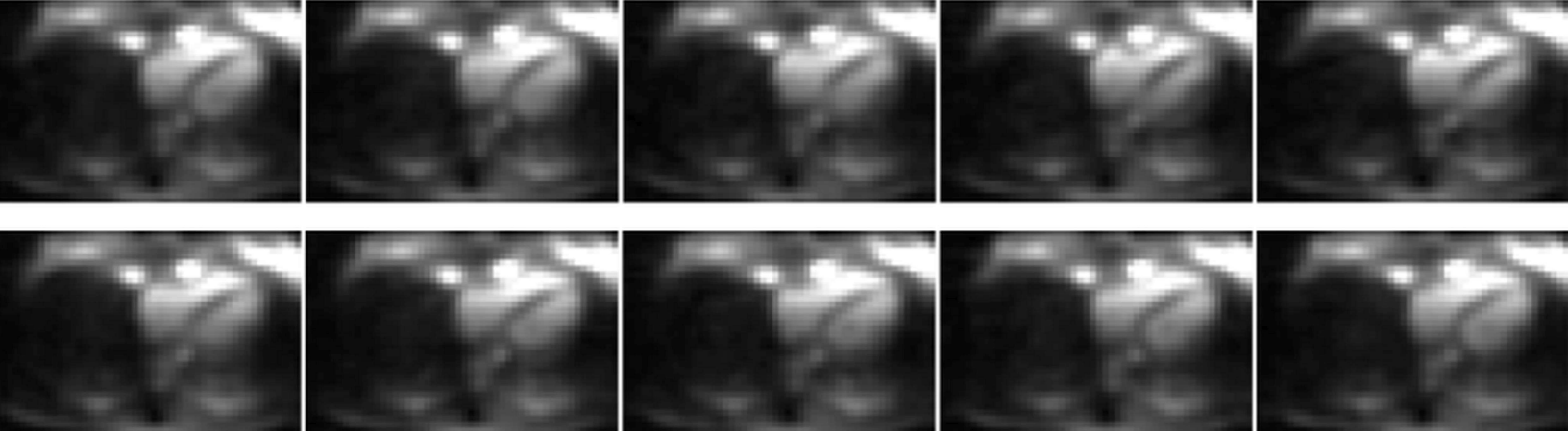

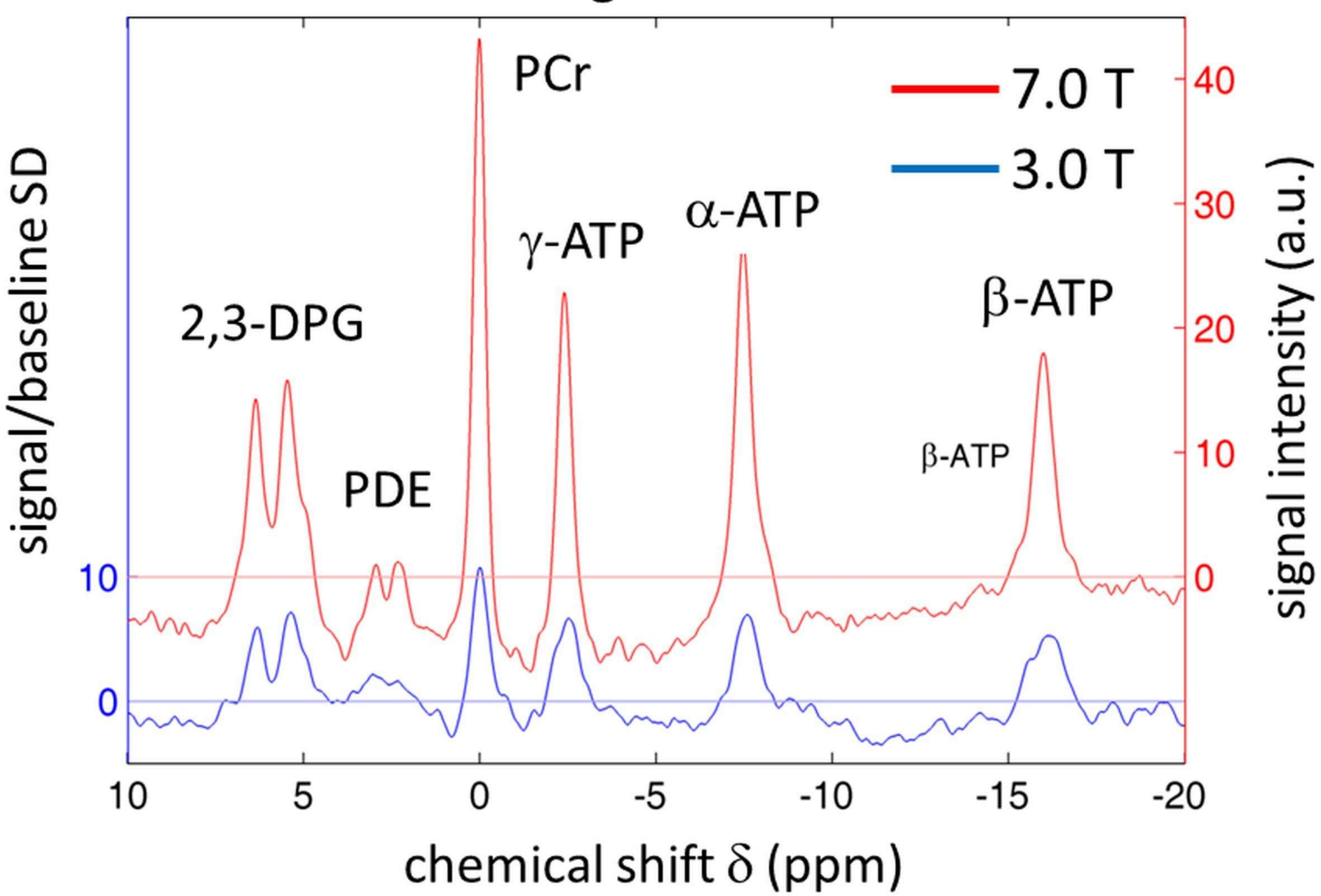
PCr
7.0 T
3.0 T
γ-ATP
α-ATP
β-ATP
2,3-DPG
PDE
β-ATP
signal/baseline SD
signal intensity (a.u.)
chemical shift δ (ppm)

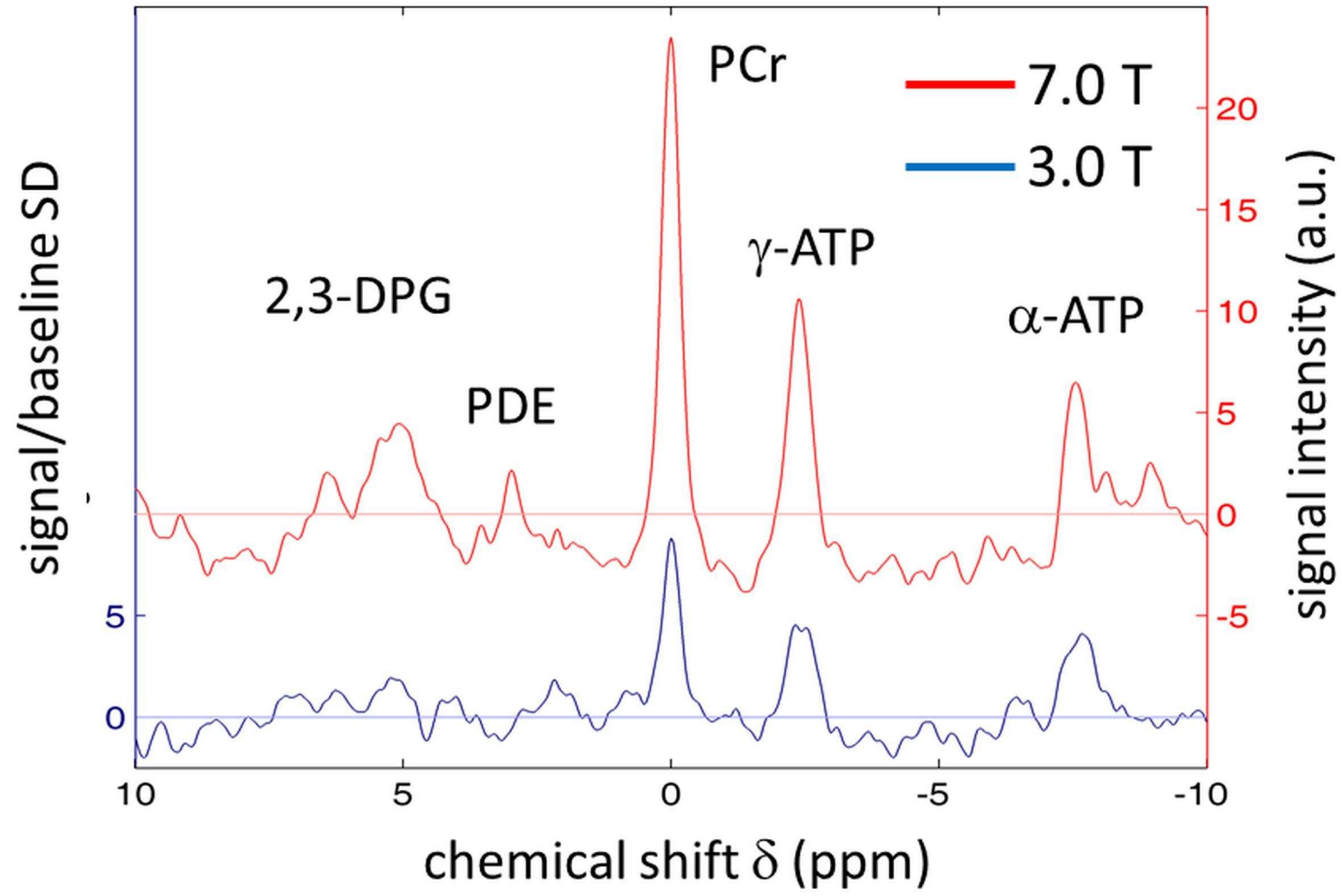
PCr
7.0 T
3.0 T
γ-ATP
α-ATP
2,3-DPG
PDE
signal/baseline SD
signal intensity (a.u.)
chemical shift δ (ppm)

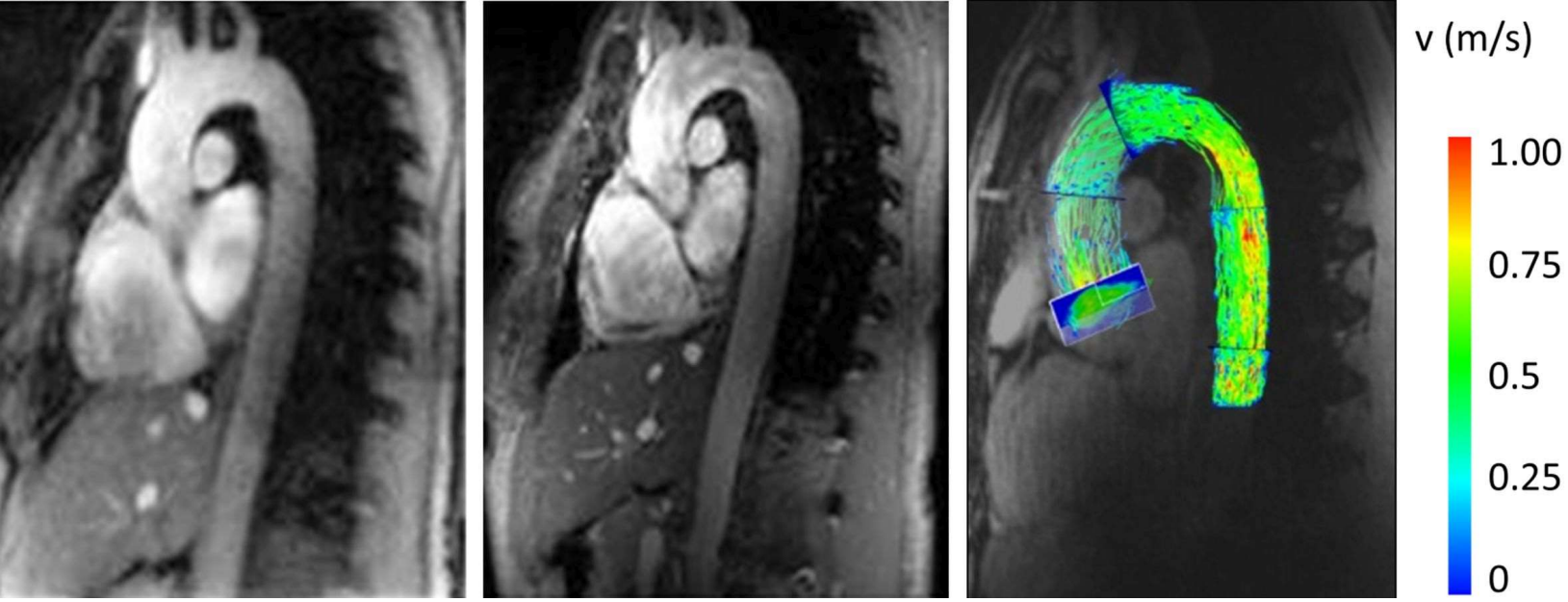
v (m/s)
1.00
0.75
0.5
0.25
0